Dalton
Transactions

Designing Nanoparticle Interfaces for Inner-Sphere Catalysis

Journal:	*Dalton Transactions*
Manuscript ID	DT-PER-03-2020-000785.R1
Article Type:	Perspective
Date Submitted by the Author:	19-Mar-2020
Complete List of Authors:	Ung, David; University of Washington, Chemistry Murphy, Ian; University of Washington, Chemistry Cossairt, Brandi; University of Washtington, Department of Chemistry

PERSPECTIVE

Designing Nanoparticle Interfaces for Inner-Sphere Catalysis

David Ung[a†], Ian A. Murphy[a†] and Brandi M. Cossairt*[a]

Received 00th January 20xx,
Accepted 00th January 20xx

DOI: 10.1039/x0xx00000x

Interfaces are an intrinsic component of nanoparticle catalysts and play a critical role in directing their function. Our understanding of the complexity of the nanoparticle interface and how to manipulate it at the molecular level has advanced significantly in recent years. Given this, attention is shifting towards the creation of designer nanoparticle interfaces that impact the activity and direct the mechanisms of inner-sphere catalytic reactions. In this perspective, we seek to highlight and contextualize these efforts. First, methods to alter nanoparticle surfaces are presented, including annealing and plasma treating, as well as more mild chemical treatments, including ligand exchange, etching, and addition (via covalent functionalization). Then interfacial chemistry developed to alter catalytic activity, selectivity, and reaction environment will be highlighted. Finally, we look forward to the challenges that remain to be overcome for realizing the true potential of colloidal nanoparticle catalysis.

Introduction

In the field of molecular catalysis, tuning chemical reactivity is not simply a matter of altering the concentration or availability of catalytic active sites. Careful design of the coordination environment surrounding the active site allows for tuning both the kinetics and mechanism of inner-sphere reactions (defined here as bond making and breaking chemistry at the active site). This is achieved through steric and electronic control of the catalytic active site as well as by introducing new reaction pathways that rely on metal-ligand cooperativity.[1] In the field of heterogeneous catalysis, on the other hand, tuning chemical reactivity and selectivity is typically achieved by altering the active sites of a pristine surface (composition control) or increasing their relative number through nanostructuring.[2] Most heterogeneous reactions of commercial relevance, however, are not carried out on pristine surfaces, but rather on small nanoparticles of a catalytic material.[2] In such cases the role of interfacial chemistry cannot be ignored given the surface area to volume scaling as these materials approach the small size limit. With the expansion of the field of colloidal nanoscience, researchers have realized the enormous potential of bottom-up colloidal synthesis of catalytically active nanomaterials. On a fundamental level, these materials can be viewed as a bridge between conventional molecular catalysts and heterogeneous surfaces (**Figure 1**). Because colloidal nanoparticles can be manipulated in solution like small molecules, and because their surfaces are necessarily passivated by organic or inorganic ligands that render them kinetically and colloidally stable,[3] it is clear that interfacial chemistry has a strong role to play in tuning material properties.

The field of colloidal nanoparticle catalysis can take inspiration from the growing literature on the surface chemistry of colloidal quantum dots and plasmonic metal nanoparticles.[3,4] For these nanoscale materials, ligands have a direct and significant impact on their function by altering their electronic structure.[5,6] As an illustrative example, and in analogy with the use of ligands to tune metal redox potentials in molecular catalysis, ligands have been shown to dramatically alter the band edge positions of quantum dots by as much as 2 eV.[7–10] Intriguingly, and of great relevance to the topic of catalysis, colloidal quantum dots and plasmonic nanoparticles are widely studied for application in photocatalytic processes that rely on energy or charge transfer mechanisms.[11] Here, ligand permeability, hydrophobicity, and charge density impact the ability for donor and acceptor species to interact through outer-sphere energy or charge transfer mechanisms. As we make the transition to the realm of colloidal nanoparticles for *inner-sphere* catalysis, the motivation for ligand-based activity control becomes even more apparent. Ligands can be used to directly tune active site availability and the inherent activity and selectivity of a given catalytic transformation. Ligands therefore offer a new dimension of parameter space with which to design catalytic interfaces. Despite this, the most frequent scheme for nanoparticle catalysis is for the nanoparticles to first be supported (or used as a powder) with ligands removed by thermal annealing or a related process.[12]

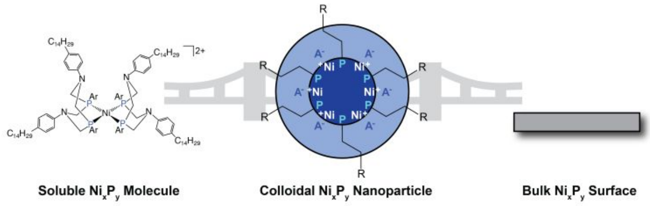

Figure 1. Colloidal nanoparticles as a bridge between soluble catalytic molecules and bulk heterogeneous surfaces.

---

[a] University of Washington, Department of Chemistry, Box 351700, Seattle, WA 98195-1700.

† These authors contributed equally.

In this perspective, we will first review methods to alter nanoparticle surfaces, including annealing and plasma treating, as well as more mild chemical treatments with a focus on materials with complex, alloyed or multicomponent lattices. We will then focus specifically on interfacial chemistry that has been developed to alter catalytic (i) activity, (ii) selectivity, and (iii) reaction environment through bulk-like interfacial effects such as surface hydrophobicity. Finally, we look forward to the challenges that remain to be overcome for realizing the true potential of colloidal nanoparticle catalysis.

Primer on Methods to Alter Nanoparticle Surfaces

Traditional schemes for altering the surface chemistry of heterogeneous catalysts are comprised almost entirely of ligand/surfactant removal. These methods are well known throughout the inorganic nanoscience community and can be loosely grouped into two classes: high-energy treatments and chemical treatments. These two approaches have drastically different influence on the chemistry of the underlying nanomaterial, which is manifested in their catalytic and/or optoelectronic applications. In this section, we will not just describe general methodology, but try to put into perspective the chemical transformations occurring at the nanocrystalline surface.

High-Energy Cleaning Methods.

Our description of thermal annealing and plasma treatments will be brief as there are already exhaustive reviews of their impact.[12–15] The fundamental concept for both approaches is to introduce sufficient energy for the cleavage of the surface-surfactant bonds and subsequent vaporization of the liberated molecular species. In the case of thermal annealing, this is accomplished by applying heat. The simplicity of this approach has made it the standard for preparing "clean" crystalline surfaces. However, the mixture of elevated temperatures and unpassivated surfaces provides the driving force for aggregation of neighboring nanocrystals, leading to the growth of larger polydisperse species.[16,17] There has been recent progress on addressing this issue by the use of low-temperature or flash annealing strategies, which can avoid the problem of agglomeration for oxidatively resistant materials.[18,19] While thermal treatments are known to be effective in removing surface ligands and are often associated with improvements in catalytic activity of nanomaterials, it has been shown that calcination does not remove all of the carbon from colloidal nanocrystal assemblies.[20] Further, the choice of annealing atmosphere (reducing or oxidizing) plays an important role in both the removal of surfactants and the alteration/passivation of the bare nanoparticle's surface.[12,21,22]

The concept of atmospheric non-innocence towards the pristine surface becomes very important when cleaning particles via plasma exposure. For this approach, the energy to liberate surfactants is supplied by high energy ions, radicals, and photon emission which decompose the ligands into smaller molecular fragments. The majority of these fragments can be liberated, but it has been shown that decomposition products can remain strongly bound to the particle surface.[23] Further, the most common and economical plasma source is oxygen, thus requiring the underlying particle to be resistant to oxidation. Recent studies have shown that plasma treatments utilizing "inert" gases like He or Ar can remove a majority of surface ligands while avoiding oxidation of the underlying particle.[24] However, bombardment by high energy ions of any species can induce random defects to form on the exposed surface facets.[25]

Although thermal and plasma annealing strategies have undoubtedly been shown to be effective in removing surface ligands, their influence on surface chemistry is known to vary largely between samples and treatment protocols. Thus, the lack of systematic understanding of the impact that these treatments have on the surface chemistry of nanoparticles should be heavily considered during experimental design and data analysis.

Chemical Ligand Exchange, Stripping, and Addition.

The unique space that nanoparticles occupy between bulk solids and discrete molecules has spurred decades of research focused on deconvoluting the complex interplay between their stable inorganic cores and dynamic organic/inorganic surfaces. In the colloidal quantum dot community specifically, these efforts have culminated in a surface ligand classification system adapted from organometallic bonding concepts. These classifications, summarized in **Figure 2**, were popularized by Owen and co-workers and will serve as the basis for our discussion on post-synthetic ligand exchange methods.[3]

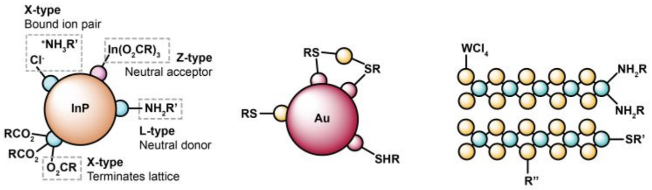

Figure 2. The coordination of different types of ligands (L-, X-, and Z-type) to a variety of inorganic nanostructures.

Just like their molecular analogues, charges must be conserved and balanced in nanocrystalline systems. Thus, the reaction mechanism for removing or altering a ligand will depend on their molecular reactivity and relationship to the surface of the particle. These initial ligand environments and the underlying particle's surface chemistry is determined by the synthetic method used to derive the particles. In a conceptual sense, the particles have a "memory" of the way in which they are formed that in-turn influences their morphology, stoichiometry, surface chemistry, and ultimately functionality. For example, most colloidally synthesized nanoparticles are capped with an X-type ligand, typically oleate or other long-chain fatty acid anion, though the specific speciation will vary by synthetic procedure. These X-type ligands are typically coordinated to excess metal cation on the surface of the particle, which is an artifact of the halted growth of nanoparticles that prevents agglomeration into larger crystals. Thus, in order to alter the native ligand environment of such a nanoparticle, one would need to employ strategies to exchange X- or Z-type ligands.

Hens and co-workers have shown that such native oleate ligands could be exchanged for protic alcohols when present in large excess.[26] The authors noted that the protic nature of the reagent was a crucial component of the exchange reaction, as protonation of the formally negative carboxylate species was required to preserve charge balance. This X-type ligand exchange has since been generalized as:

Eq. 1 $[\mathrm{NP}]\text{—}\mathrm{X} + \mathrm{HY} \rightleftarrows [\mathrm{NP}]\text{—}\mathrm{Y} + \mathrm{HX}$

However, it is important to note that ligand exchange is actually an equilibrium process. The same study found that over time the desorbed oleate ligands would rebind. This equilibrium can be shifted by factors like concentration, denticity, and pKa. This concept has been shown by our group and others through monitoring the exchange of native oleate ligands for other organic acids.[27–30] Through these studies it was found that phosphonic acids readily displace carboxylic acids and effectively bind irreversibly due to both their low pKa and multidentate binding modes. This straightforward method to replace native X-type ligands is not limited to acids, but also applies to halides, pseudohalides, and strong bases.[31–34] Though, when planning ligand exchange reaction conditions, be mindful that some colloidal nanocrystals are not stable in strongly acidic or basic conditions and will either etch or completely dissolve.

As mentioned above, X-type ligands with a formal negative charge neutralize the formally positive charge of excess cations that passivate the particle surface. In fact, it is generally understood that, especially for smaller particles, the surface is often terminated by a layer of excess metal cation coordinated by anionic ligand.[35,36] This is commonly studied by inductively coupled plasma mass spectroscopy (ICP-MS) that show a super-stoichiometric concentration of metal species in as-synthesized materials. These effectively neutral Lewis-acidic ligand complexes are referred to as Z-type ligand. Because these complexes are effectively neutral, ligand exchange reactions must employ other Z-type complexes or formally neutral Lewis-basic species known as L-type ligands (**Figure 3**).[36,37] These ligand exchange reactions can also be generalized according the following equations:

Eq. 2 $[\mathrm{NP}]\text{—}\mathrm{M_1X} + \mathrm{M_2Y} \rightleftarrows [\mathrm{NP}]\text{—}\mathrm{M_2Y} + \mathrm{M_1X}$

Eq. 3 $[\mathrm{NP}]\text{—}\mathrm{MX} + 2\mathrm{L} \rightleftarrows [\mathrm{NP}]\text{—}\mathrm{L} + \mathrm{LMX}$

In their study, Owen and co-workers thoroughly investigated the complex equilibrium of these exchange reactions and found that the efficacy of ligand exchange was roughly a function of the relative Lewis-basicity of L.[36] They showed that although alcohols, phosphines, and amines were all able to displace some amount of MX_n, short-chain primary amines were the most effective. Further, the efficacy of primary amines was improved by the simultaneous addition of a chelating diamine species. They propose this is due to an increased stabilization of the desorbed L_yMX_n species, coupled with stabilization of the particle surface. Though amines are generally effective species for surface passivation, the real affinity for ligand binding is dictated by individual atomic preferences that can be described by hard soft acid base theory. As such, binding strength will vary with the specific speciation of a system. Because of this, exchange between L-type ligands can also be driven by this difference in intrinsic binding affinity, according the general equation:

Eq. 4 $[\mathrm{NP}]\text{—}\mathrm{L_1} + \mathrm{L_2} \rightleftarrows [\mathrm{NP}]\text{—}\mathrm{L_2} + \mathrm{L_1}$

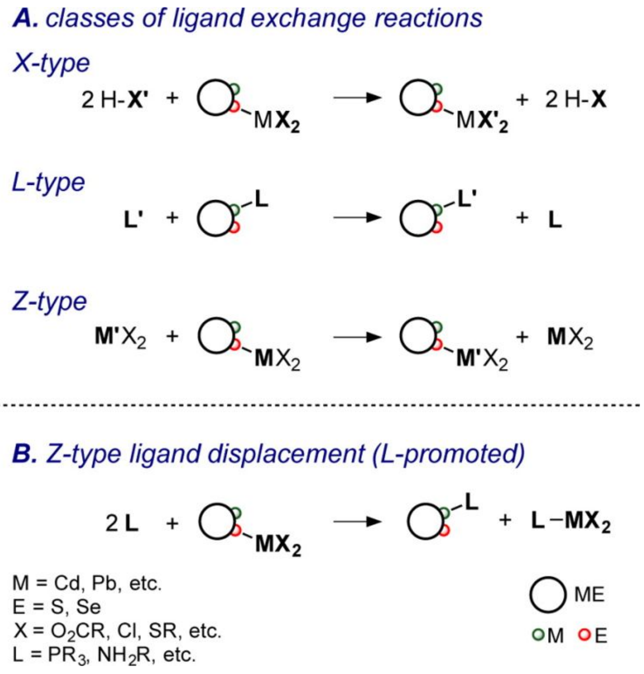

Figure 3. Schematic depiction of X-, L-, and Z-type ligand exchange reactions for Cd and Pb chalcogenide model systems. Reprinted with permission from N. C. Anderson, M. P. Hendricks, J. J. Choi, J. S. Owen. *Journal of the American Chemical Society*, 2013, **135**, 18536 – 18548. Copyright 2013 American Chemical Society.

In addition to the conventional ligand exchange methods presented above, chemical ligand stripping to terminate the lattice with weakly or non-coordinating anions is being increasingly pursued. Alkylating agents (i.e., $R_3O^+X^-$, **Eq. 4**) and nitrosonium salts ($NO^+BF_4^-$) can displace the native ligand while reacting to form a neutral species with little binding affinity for the particle surface. The positive charge remaining on the surface of the particle is then neutralized by the counter anion, such as BF_4^-.[38–40] The resulting particles can be soluble in polar solvents, remain monodisperse, retain crystallographic integrity, and can act as blank templates to be re-ligated by other species.[39–41]

Eq. 4 $[\mathrm{NP}]\text{—}\mathrm{X} + \mathrm{R_3O^+Y^-} \rightarrow [\mathrm{NP}]^+\mathrm{Y^-} + \mathrm{R}\text{—}\mathrm{X} + \mathrm{R_2O}$

Irreversible ligand stripping by the methods mentioned above can also cause some confusion without a rational understanding of the system. For example, if both ligands and excess cations are desorbed from the surface, the particles become more stoichiometric and develop a balanced charge, thus losing colloidal stability. This can generally be avoided by carrying out reactions in polar, coordinating solvents like DMF that can act as L-type ligands that colloidally stabilize the neutral particles.[42] Still, the complex nature of ligand environment and colloidal stability have pushed researchers to develop other, softer and more reversible, ligand stripping procedures. To this end, Helms and co-workers explored the viability of Lewis-acid-base adducts for X-type ligand removal, but not deactivation.[43] In this study, they showed that oleate ligands could be displaced by BF_3:DMF, according to the following general equation:

Eq. 5 $[NP]—X + LA:LB \rightleftarrows [NP]^{+}[LA:X]^{-} + LB$

This weak electrostatic attraction between the $[LA:X]^{-}$ adduct and the charged particle surface allowed the particles to retain colloidal stability while still providing a malleable template to further alter surface functionality (**Figure 4**).

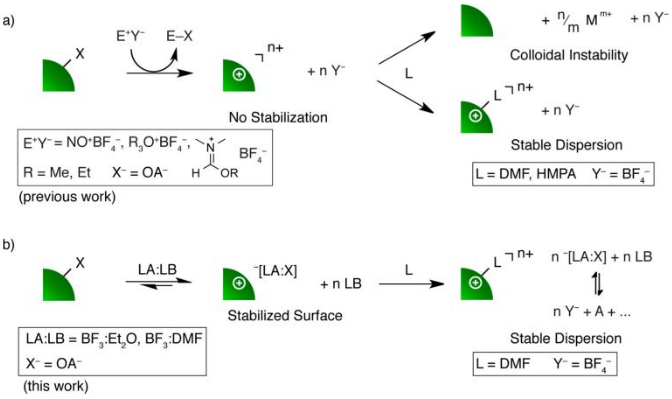

Figure 4. Schematic depiction of **a**) irreversible ligand stripping with strong electrophiles and **b**) reversible ligand stripping with Lewis acid-base adducts. Abbreviations: X^{-} = anionic ligand, E^{+} = electrophile, Y^{-} = non-coordinating anion, M^{n+} = metal ion, LA:LB = Lewis acid−base adduct, L = charge-neutral coordinating solvent (e.g., DMF). For sensitive NC compositions, loss of M^{n+} from the surface leads to colloidal instability, particularly when repassivation of surface M^{n+} by L is not competitive with M^{n+} desorption. The dynamic exchange of $[LA:X]^{-}$ on and off the NC differentiates stripping under equilibrium control from earlier approaches. In the approach described herein, Y^{-} is generated through disproportionation of $[LA:X]^{-}$ as described in the main text. Reprinted with permission from S. E. Doris, J. J. Lynch, C. Li, J. J. Urban, B. A. Helms. *Journal of the American Chemical Society*, 2014, **136**, 15702 – 15710. Copyright 2014 American Chemical Society.

Depending on the nanomaterials' desired application, full ligand removal for a bare surface may not be necessary. For example, native long chain surface ligands are often a detriment to nanomaterials in electronic applications because of the highly insulating aliphatic tails. Completely removing these surfactants through chemical or thermal treatments may improve electronic communication but can also lead to aggregation of the particles. Rather than full ligand removal, these insulating ligands can be exchanged with compact halide (**Eq. 6**),[41,44,45] psuedohalide (N_3^{-}, CN^{-}, SCN^{-}, etc.),[33,46] or molecular metal chalcogenides.[32,34,46,47] These compact surfactants behave as X or Z-type surface ligands, but can greatly increase the electronic communication between nanoparticles and with the local environment when compared to the native aliphatic ligands.

Eq. 6 $[NP]—X + TMS—Y \rightarrow [NP]—Y + TMS—X$
(TMS = trimethylsilyl)

Depending on the type of nanomaterial employed for catalysis, sites for modifying ligand chemistry using coordinate-covalent bonding may not be readily accessible. In these cases, covalent surface modification by forging new main group-main group bonds is a desirable approach. Here we can take the transition metal dichalcogenide MoS_2 as an illustrative example. There are many methods to functionalization this layered material depending on the starting crystal phase.[48] When in the semiconducting 2H phase, the basal planes are considered chemically inert, meaning reactions can only occur at edge and defect sites. When defects are the only accessible reactive site, functionalization is limited to an approach known as "ligand conjugation".[49,50] Ligand conjugation requires a terminal thiol moiety on the functional ligand to react at S-vacant defect sites. It is proposed that the S from the thiol group bonds with the under coordinated Mo atoms, thus embedding the ligand into the edges of the 2D sheet - however the exact mechanism of S-R integration is still under investigation. Although the basal planes are inert in the semiconducting 2H phase, once converted to the metallic 1T phase by exfoliation with alkali metals (usually n-butyllithium) they become quite reactive. It has been shown that in this more reactive polymorph the basal plane S atoms are susceptible to electrophilic addition by diazonium salts[51,52] and organoiodine precursors (**Figure 5a**).[53,54] This concept of having reactive electrons with a suitably reducing potential accessible to the reaction site is becoming known as a critical factor in driving covalent functionalization. Recently, Lewis and co-workers explored this idea by adding extra metallocene reductants to a reaction mixture of iodoalkyl species and alkylated MoS_2-R sheets (**Figure 5b**).[55] They found that the extent of functionalization could be pushed past that accessible by exfoliation with n-butyllithium alone, validating previous studies which postulated that the covalent functionalization was self-limited by the negative charges localized on the sheets after exfoliation. Further, their study showed that the potential of the reductant also played a role in increasing functionalization, where a stronger reductant like cobaltocene induced more functionalization than a weaker reductant like ferrocene.

While we have highlighted the covalent functionalization of MoS_2 here, this type of surface modification can be applied to a wide variety of nanomaterials including carbons and black phosphorus,[56–58] as well as non-layered materials like transition metal phosphides and main-group metal sulfides to alter their physical and electronic structure, and in turn their catalytic activity. It is notable, however, that there is a significant difference in total content and the level of detail found in the literature on the topic of covalent functionalization in comparison to dative ligand interactions. Covalent surface modification is an emerging and rapidly developing field, requiring further exploration into both synthetic methods and the effects that covalent functionalization has on the electronic/structural properties of the underlying material.

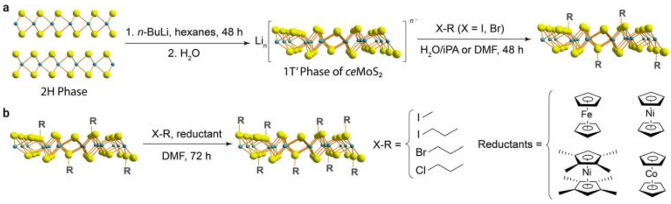

Figure 5. a) Conversion of 2H phase to 1T by exfoliation with n-butyllithium followed by conditions for self-limited alkylation with alkylhalide reagents. **b**) Procedure for further reductant activated alkylation of functionalized MoS_2 sheets. Reprinted with permission from E. X. Yan, M. Cabán-Acevedo, K. M. Papadantonakis, B. S. Brunschwig, N. S. Lewis. *ACS Materials Letter*s, 2020, **2**, 133 – 139. Copyright 2020 American Chemical Society.

Tuning Nanoparticle Catalyst Activity Using Surface Chemistry

As discussed in the previous section, typical surface ligands for colloidally synthesized nanomaterials are comprised of long hydrocarbon chains with polar head groups that bind to the material via dative/coordinate-covalent bonds. For example, long chain carboxylates, amines and related ammonium salts, phosphines, and thiolates have all been used as common surfactants for nanomaterials. The long hydrocarbon chains prevent aggregation of the nanoparticles through steric stabilization and provide solubility in common nonpolar solvents, while the polar head groups bind and stabilize the highly energetic surface of the nanomaterials or provide a site for electrostatic stabilization through charge localization. These surface ligands are typically considered a detriment to catalysis due to the blocking of active sites and are commonly removed via thermal or chemical treatments as described above. However, recent work has shown that these coordinate-covalent bonding surface ligands, in addition to the emerging classes of covalent functional groups, can be used as a synthetic lever to tune the reactivity of catalysts by modifying the electronic structure of a nanocrystal or by adjusting its interaction with substrates.

Activity.

Nanoparticles occupy a unique regime between molecules and bulk materials. Similar to how ligands play a large role in the electronic structure of molecular coordination complexes, surface ligands can alter the electronic structure of nanoparticles and influence their behavior even though they can be hundreds to thousands of atoms in size. These changes in electronic structure can have large impacts on the binding strength of reaction intermediates, which in turn can impact the activity of a catalyst due to many of these transformations following a volcano plot behavior, via the Sabatier principle.[59,60] In many cases these ligand effects on electronic structure follow typical chemical design principles, such as inductive effects. For example, increasing the chain length of an alkylthiolate surface ligand on Au nanoparticles increases the charge density in the core, which thereby increases the Fermi level of the nanomaterial (**Figure 6**).[61] The extent in which the surface ligands influence the electronic structure can be affected by the size of the nanomaterial. Smaller nanomaterials have intrinsically higher ratios of surface atoms, and therefore the ligand-induced electronic effects on catalytic activity may be more prominent than for larger systems. This size-dependent ligand effect has been shown in Au nanomaterials where porphyrin-protected Au clusters (<2 nm) have a much larger enhancement in electrocatalytic HER activity compared to the larger 2.2 and 3.8 nm Au nanoparticles.[62]

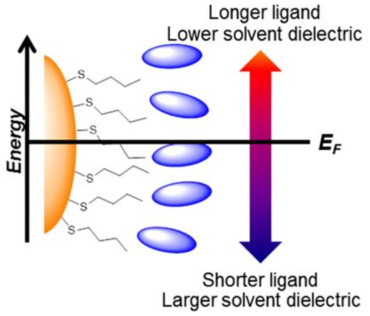

Figure 6. Increasing tail length of alkanethiolate surface ligands increases fermi level of Au nanoparticles. Reprinted with permission from A. Cirri, A. Silakov, L. Jensen, B. J. Lear. *Journal of the American Chemical Society,* 2016, **138**, 15987 – 15993. Copyright 2016 American Chemical Society.

Traditionally, surface ligands tend to be bound to the nanomaterial via dative or electrostatic interactions as a consequence of the colloidal methods used to make them. However, there has been increasing interest in the covalent functionalization of nanomaterials, with 2D nanomaterials laying the foundation as described in the previous section. Focusing on a study examining catalytic activity, Miller and co-workers have shown that MoS_2 nanosheets can be covalently functionalized with a range of diazonium reagents (**Figure 7**).[52] By tuning the Hammett parameter of the substituent on the phenyl ring, the authors were able to adjust the electron density on the nanomaterial and vary its reactivity, which influences its electrocatalytic activity for HER. This method of introducing covalently bound surface ligands allows for strong ligand-nanomaterial interactions and can be used to tune the reactivity and stability of nanomaterial catalysts.

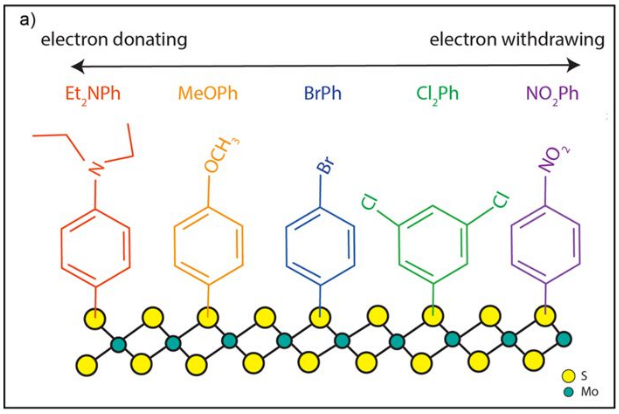

Figure 7. Covalently functionalizing nanomaterial surfaces allows for strong ligand interactions and can be used to tune the reactivity and stability of the material. Reprinted with permission from E. E. Benson, H. Zhang, S. A. Schuman, S. U. Nanayakkara, N. D. Bronstein, S. Ferrere, J. L. Blackburn, E. M. Miller. *Journal of the American Chemical Society,* 2018, **140**, 441 – 450. Copyright 2018 American Chemical Society.

A unique approach to tuning the electronic structure of nanoparticles for heterogeneous catalysis is using surface-anchored organic ligands on a support that has a terminal binding group. These dative interactions with deposited nanoparticles can modify the electronic structure, as shown in the case of Pd nanocrystals on a TiO_2 photocatalyst support for photocatalytic hydrogen peroxide production.[63] In this example, the dative interaction between a TiO_2-anchored amine on the Pd nanocrystal improves the overall photocatalytic activity of the whole system (**Figure 8**). The amines donate electron density into the Pd nanoparticle, modifying the electronic structure such that the charge separation onto the TiO_2 support is improved, as well as enhancing the intrinsic activity and selectivity of the Pd nanocrystals for ORR to form the H_2O_2 product..[63]

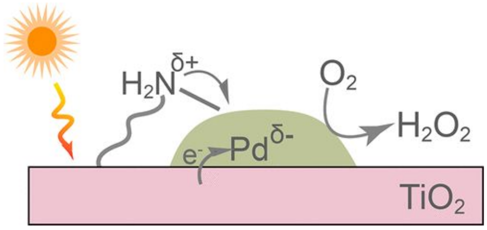

Figure 8. Surface anchored organic ligands on the support can be used to adjust the electronic structure of the nanomaterial catalyst. Reprinted with permission from C. Chu, D. Huang, Q. Zhu, E. Stavitski, J. A. Spies, Z. Pan, J. Mao, H. L. Xin, C. A. Schmuttenmaer, S. Hu, J.-H. Kim. *ACS Catalysis,* 2019, **9**, 626 – 631. Copyright 2019 American Chemical Society.

Electronic structure effects can be used to rationally design nanoparticle interfaces to tackle common problems in catalysis, such as the poisoning of active sites. One of the major barriers to effective catalysis is strongly binding intermediates preventing the active site from turning over (**Figure 9**). For example, even though Pt is among the most active single metal catalysts for the oxygen reduction reaction (ORR), its remaining overpotential is linked to the strong adsorption of oxygen and hydroxyl intermediates on the surface.[64] Strongly adsorbing surface ligands on Pt nanoparticles have generally thought to have been detriments to ORR catalysis, but small amounts of amines coordinated to the surface of carbon-supported Pt nanoparticles have been shown to improve electrochemical reactivity even with decreased electrochemically active surface area (ECSA).[64] This is a key discovery because the typical explanation for improved activity through surface ligand removal is increased surface area and therefore the number of active sites. The presence of amine surface ligands on Pt has been shown to shift the frontier d-band structure, which in turn alters the free energy of adsorption (ΔG_{ad}) and the surface coverage of intermediates on the surface of Pt. Sung and co-workers have shown that this change in ΔG_{ad} weakens the adsorption of oxygen and hydroxyl groups on the surface of Pt, preventing the strong binding of reaction intermediates and improving the overall reactivity of the catalyst.[64]

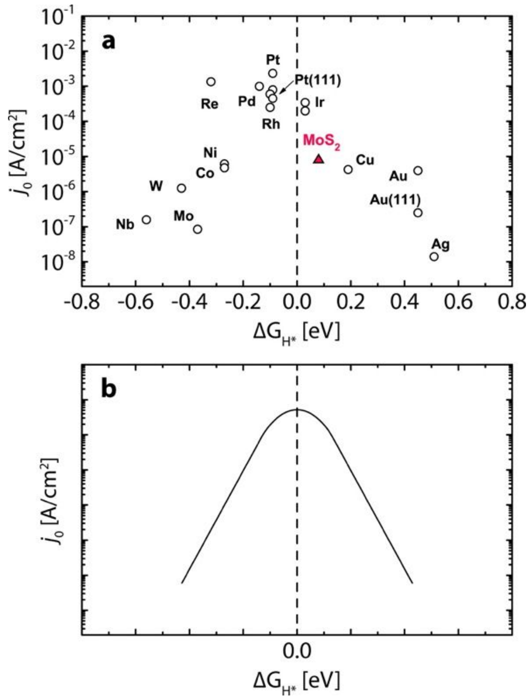

Figure 9. Volcano plots (experimental, **a** and theoretical, **b**) are a manifestation of the Sabatier principle and are commonly invoked to describe catalytic activity. Materials on either end of the volcano plot either bind the intermediate too strongly or too weakly and this limits turnover. Surface ligands may be utilized to adjust the strength of the binding of required reaction intermediates. Reprinted with permission from J. D. Benck, T. R. Hellstern, J. Kibsgaard, P. Chakthranont, T. F. Jaramillo. *ACS Catays*is, 2014, **4**, 3957 – 3971. Copyright 2014 American Chemical Society.

Adsorption of poisonous spectator species onto the surface can prevent the formation of required surface intermediates and hinder active site turnover, such as PO_4^{3-} on Pt for the ORR.[64,65] H_3PO_4-doped polybenzimidazole (PBI) membranes have been highly studied for proton exchange membrane fuel cells

(PEMFCs) because they show improved reactivity and stability at elevated temperatures. However, one major concern for these systems is the competitive adsorption and poisoning of the surface of Pt by PO_4^{3-} anions. Jang and co-workers have illustrated that the native oleylamine surface ligands on Pt nanoparticles enable the "third-body effect," in which the oleylamine surfactants block the poisonous spectator PO_4^{3-} anions from binding to the surface (**Figure 10**).[65]

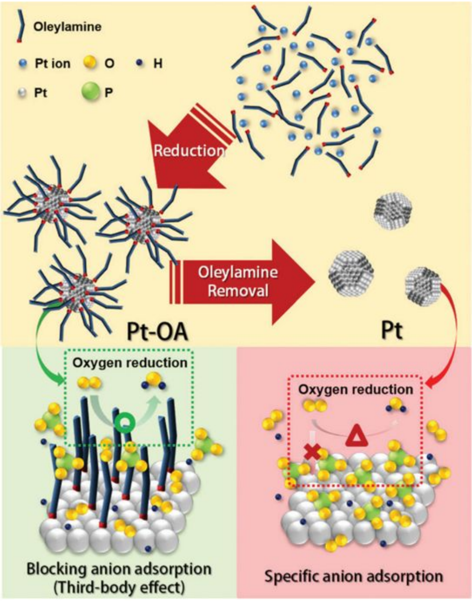

Figure 10. Oleylamine on the surface of Pt blocks poisonous PO_4^{3-} adsorption on the catalytically active surface via the "third-body effect". Reproduced from Ref. 65 with permission from The Royal Society of Chemistry.

Selectivity.

Another major barrier to efficient catalysis is the presence of competing side reactions. This is particularly relevant for the CO_2 reduction reaction (CO_2RR), where selectivity is a central challenge both in targeting a single carbon-containing product and minimizing competition from the hydrogen evolution reaction (HER) due to the necessary presence of protons in the reaction solution. Recent work done by Hwang and co-workers have shown that the tendency of a Ag nanocrystal catalyst to participate in CO_2RR or HER can be modulated with the use of surface ligands.[66] Amine-capped Ag nanocrystals have almost 100% faradaic efficiency for the reduction of CO_2 to CO. However, using a thiol surface ligand actually increases the HER activity and reduces the CO_2RR faradaic efficiency. DFT calculations were used to show that the presence of amine surface ligands improves the binding energy of COOH intermediates while destabilizing adsorbed H intermediates. Conversely, thiol surface ligands improve ΔG_{ad} for both COOH and H intermediates and therefore participates in competitive CO_2RR and HER, reducing the faradaic efficiency for the CO_2RR.[66]

Similar selectivity has been promoted on cysteamine-capped Au nanoparticles for CO_2RR. The sulfur end of the cysteamine ligand binds to the surface of Au nanoparticles and alters the electronic structure of the surface while the terminal amine group on cysteamine is able to participate in a cooperative ligand mechanism by chemisorbing CO_2 and stabilizing its relevant adsorbed intermediates.[67] This lowers the overpotential and improves the faradaic efficiency of Au nanocrystals for electrocatalytic CO_2 reduction to CO.[67]

There has also been work done with "designer" surface ligands on Au nanoparticles with n-heterocyclic carbenes (NHCs). Using the strongly sigma-donating NHCs as surface ligands for Au nanoparticles has been shown to improve the faradaic efficiency of CO_2 reduction as well as changing the mechanistic pathway by changing the rate-determining step (**Figure 11**).[68]

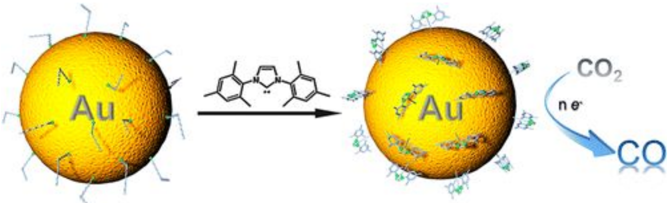

Figure 11. Utilizing "designer" NHCs to improve the faradaic efficiency of CO_2 reduction to CO. Reprinted with permission from Z. Cao, D. Kim, D. Hong, Y. Yu, J. Xu, S. Lin, X. Wen, E. M. Nichols, K. Jeong, J. A. Reimer, P. Yang, C. J. Chang. *Journal of the American Chemical Society,* 2016, **138**, 8120 – 8125. Copyright 2016 American Chemical Society.

Selectivity also becomes an issue when considering the extent of a reaction. For example, using Pt or Co/Pt nanoparticle catalysts for selective hydrogenation of an alkyne to an alkene can often fully hydrogenate to produce the saturated alkane product. Shevchenko and co-workers have shown that primary amines can be used to tune the selectivity of 4-octyne hydrogenation to 4-octene from 0% to greater than 90% depending on the amine coverage on the surface of the nanoparticle (**Figure 12**).[69] At high amine coverage, the binding energy of the amine is higher than that of the alkene intermediate, preventing the alkene from reacting with the catalytically active surface to form the undesired alkane product.[69]

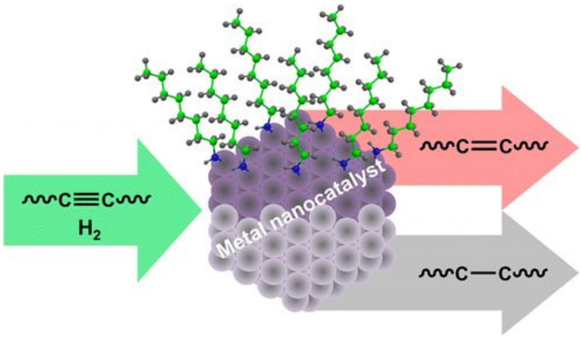

Figure 12. Surface ligands can be utilized to adjust the extent of hydrogenation with metal nanocrystal catalysts. Reprinted with permission from S. G. Kwon, G. Krylova, A. Sumer, M. M. Schwartz, E. E. Bunel, C. L. Marshall, S. Chattopadhyay, B. Lee,

J. Jellinkek, E. V. Shevchenko. *Nano Letters,* 2012, **12**, 5382 – 5388. Copyright 2012 American Chemical Society.

Altering the outer-coordination sphere interactions of the nanoparticle surface with the solvent can also assist in tuning the selectivity of an electrocatalyst. Buonsanti and co-workers have shown that imidazolium ligands can be used to tune selectivity of Ag nanoparticles for CO_2RR when competing with HER.[70] They illustrate that the changes to the electronic structure of the Ag nanocrystal plays a small role in the catalyst performance, and that the length of the hydrocarbon tail plays an important role in balancing the steric properties of the surface with the hydrophobicity, which allows CO_2 to interact with the substrate but limits the amount of H_2O to prevent competitive HER.[70]

Extra-Particle Effects.

Modifying the surface of a nanocrystal catalyst and its synergy with substrate is an obvious component in overall catalytic activity, but a less intuitive factor to catalytic performance is the interface of the catalyst with bulk solvent (and the electrolyte in the case of electrocatalysis). Whether the nanocrystals are colloidally suspended in solution or if they are immobilized onto a heterogeneous support, the surface ligands define the interface between the nanocrystal and solvent. Kimber and co-workers have shown via x-ray pair distribution function analysis that both polar and nonpolar solvents restructure around nanoparticles. This result shows that nanoparticles in solution have a solvation shell that can impact its reactivity. The characteristics of the nanoparticle-solvent interface may greatly alter the catalytic activity of nanocrystals by altering the interactions with the bulk solvent.[71]

Recent work from our lab has shown that the removal of long chain carboxylate and amine surface ligands on CoP greatly improves overpotential for HER due to the improved hydrophilicty of the film (**Figure 13**). The improved wettability of the electrode film increases electrochemically active surface area (ECSA) because there is no longer a hydrophobic interface preventing the electrolyte solution from interaction with the electrode surface.[40] The hydrophobicity of an interface has also been shown to play a role in the oxygen evolution reaction (OER), where phosphorylation of a NiFe hydroxide film greatly improves the electrocatalytic activity. The phosphorylation increases the ECSA due to improved wettability of the electrolyte solution with the surface of the catalyst.[72]

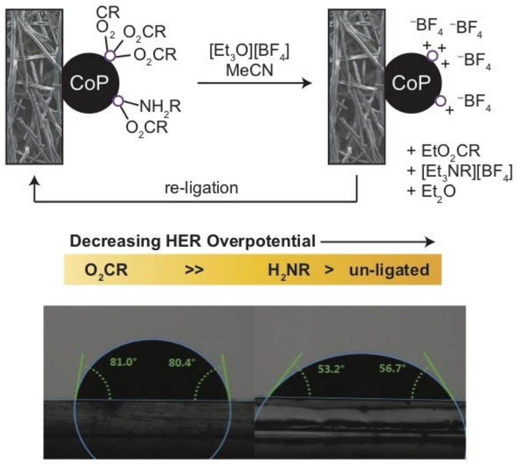

Figure 13. Long chain surface ligands on CoP impede electrocatalytic HER by generating a hydrophobic interface. Removing the surface ligands improves the interface with the electrolyte solution in aqueous conditions. Adapted with permission from D. Ung, B. M. Cossairt. *ACS Applied Energy Materials,* 2019, **2**, 1642 – 1645. Copyright 2019 American Chemical Society.

Surface ligands can also imbue cooperative ligand effects by interacting with the substrate. For example, certain bifunctional surface ligands have been shown to participate as proton relays and increase the local concentration of protons at the surface of a nanocrystal catalyst. Ethylenediamine functionalized NiMo electrocatalysts have improved HER activity in aqueous alkaline conditions when compared to primary amines. The presence of the terminal amine at the interface of the catalyst and the electrolyte solution improves the adsorption of water molecules and their transportation to the catalyst surface.[73] This improvement in catalytic activity with improved local concentration of substrate can also be seen with polymer-based surface ligands, such as polyethylenimine or polyallylamine. In the case of polyallylamine, Chen and co-workers have shown that Pt tripods have an onset overpotential that is more positive than the theoretical value of HER in aqueous acidic conditions (0 V vs RHE) because the local proton concentration is increased by orders of magnitude compared to the bulk electrolyte solution.[74,75] Functionalization with cooperative ligands for catalysis acts as a local modification to surface atoms that are able to interact with the substrate. Because of this local effect, these ligands can play a critical role in enhancing catalytic activity for inner-sphere electron transfer transformations, regardless of the size of the nanomaterial.

Conclusions

The full potential of nanoscale catalysts will only be realized once we have mastered the manipulation of their interfacial chemistry. To date, only scattered reports of utilizing nanoparticle surface chemistry to alter catalyst activity, selectivity, and extra-particle interactions have been documented. We need to be more systematic in our approach to deduce generalizable design principles for interfacial design. As a community we must study how surface modification impacts inner-sphere reactions and overall reaction landscapes. This will require thinking about heterogeneous active sites as truly molecular entities characterized by bonds being made and broken in an atomically defined manner. Only then will we be able to harness the power of interfacial design in heterogeneous catalysis that has so well served the natural evolved world of biological enzymes and the man-made world of organometallic chemistry. Theoretical studies have been used extensively to probe inner-sphere chemistry,[76–78] but complementary experimental data are lacking. A recent example from the Center for Molecular Electrocatalysis demonstrates the insight that can come from such measurements.[79] On the basis of the reactivity of CoP with various molecular hydrogen donating and accepting reagents, the distribution of binding free energies for H atoms on CoP (both mesoscale particles and colloidal nanoparticles) was estimated to be roughly 51–66 kcal mol^{-1} ($\Delta G°_H \cong 0$ to -0.7 eV vs H_2). These results highlight the complexity of these surfaces and illustrate that the numbers extracted from calculations on pristine surfaces are an oversimplification.

In order to truly utilize interfacial design for improved catalytic activity, the nanomaterial surface needs to be stable in the desired catalytic conditions. But due to the dynamic nature of coordinate-covalent bonds typified by traditional surface ligands (e.g. carboxylates, amines, etc.), highly engineered interfaces designed to modify activity will evolve over time. For example, HER catalysts typically have the greatest activity in highly acidic electrolyte conditions. However, datively bound carboxylate and amine surface ligands commonly found on colloidally prepared nanomaterials can be easily protonated and removed from the nanomaterial surface. Similarly, ORR catalysts typically have the best performance in highly alkaline electrolyte conditions. But the high concentration of OH^- can displace the surface ligands on the engineered interface by altering the equilibrium or by etching the Z-type ligands on the surface. Of course, this is a problem in the molecular catalysis field as well – ligand displacement under catalytic conditions leads to the formation of uncontrolled nanoparticles or worse, complete catalyst deactivation. We posit that the best method towards designing stable interfaces that can be utilized for improved catalysis in a variety of systems is through covalent modification. Formally covalent bonds between the nanoparticle surface and new surface ligands should be much more stable and less dynamic in the catalytic environment. However, these covalent bonding interactions alter material structure and properties in ways that are largely as yet unknown. Exciting recent examples of this approach can be found in the carbon literature where the covalent modification of graphite has led to novel insight into reaction mechanisms and improved catalyst activity (**Figure 14**).[80–82] We believe this covalent approach to heterogeneous surface modification, including at complex nanoparticle interfaces, will have broad implications for the molecular-level design of next-generation catalytic systems.

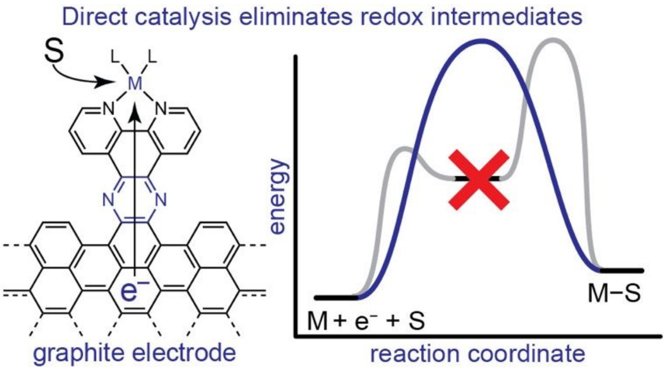

Figure 14. The covalent coupling of a molecular hydrogen evolution catalyst to a graphitic electrode eliminates stepwise pathways and forces concerted electron transfer and proton binding. Reprinted with permission from M. N. Jackson, C. J. Kaminsky, S. O. Oh, J. F. Melville, Y. Surendranath. *Journal of the American Chemical Society,* 2019, **141**, 14160 – 14167. Copyright 2019 American Chemical Society

Conflicts of interest

There are no conflicts to declare.

Acknowledgements

This work was supported as part of the Center for Molecular Electrocatalysis, an Energy Frontier Research Center funded by the U.S. Department of Energy, Office of Science, Office of Basic Energy Sciences. D. U. and I. A. M. were supported in part through a fellowship from the University of Washington Clean Energy Institute.

Notes and references

1 D. Steinborn and A. Harmsen, *Fundamentals of Organometallic Catalysis*, John Wiley & Sons, Inc, 2011.
2 R. A. van Santen, *Modern Heterogeneous Catalysis*, John Wiley & Sons, 2017.
3 J. S. Owen, *Science*, 2015, **347**, 615–616.
4 E. Pensa, E. Cortés, G. Corthey, P. Carro, C. Vericat, M. H. Fonticelli, G. Benítez, A. A. Rubert and R. C. Salvarezza, *Acc. Chem. Res.*, 2012, **45**, 1183–1192.
5 M. A. Boles, D. Ling, T. Hyeon and D. V. Talapin, *Nature Mater.*, 2016, **15**, 141–153.
6 P. Liu, R. Qin, G. Fu and N. Zheng, *J. Am. Chem. Soc.*, 2017, **139**, 2122–2131.
7 P. R. Brown, D. Kim, R. R. Lunt, N. Zhao, M. G. Bawendi, J. C. Grossman and V. Bulović, *ACS Nano*, 2014, **8**, 5863–5872.
8 C.-H. M. Chuang, P. R. Brown, V. Bulović and M. G. Bawendi, *Nature Mater.*, 2014, **13**, 796–801.
9 D. M. Kroupa, M. Vörös, N. P. Brawand, B. W. McNichols, E. M. Miller, J. Gu, A. J. Nozik, A. Sellinger, G. Galli and M. C. Beard, *Nature Commun.*, 2017, **8**, 15257.
10 B. P. Bloom, L.-B. Zhao, Y. Wang, D. H. Waldeck, R. Liu, P. Zhang and D. N. Beratan, *J. Phys. Chem. C*, 2013, **117**, 22401–22411.
11 E. A. Weiss, *ACS Energy Lett.*, 2017, 1005–1013.
12 Z. Niu and Y. Li, *Chem. Mater.*, 2014, **26**, 72–83.

13 L. M. Rossi, J. L. Fiorio, M. A. S. Garcia and C. P. Ferraz, *Dalton Trans.*, 2018, **47**, 5889–5915.
14 M. Nitschke, *Polymer Surfaces and Interfaces: Characterization, Modification and Applications*, ed. M. Stamm, Springer, Berlin, Heidelberg, 2008.
15 Thermal Annealing - an overview | ScienceDirect Topics, https://www.sciencedirect.com/topics/engineering/thermal-annealing, (accessed February 28, 2020).
16 S. J. Baik, K. Kim, K. S. Lim, S. Jung, Y.-C. Park, D. G. Han, S. Lim, S. Yoo and S. Jeong, *J. Phys. Chem. C*, 2011, **115**, 607–612.
17 A. W. Wills, M. S. Kang, A. Khare, W. L. Gladfelter and D. J. Norris, *ACS Nano*, 2010, **4**, 4523–4530.
18 M. Cargnello, C. Chen, B. T. Diroll, V. V. T. Doan-Nguyen, R. J. Gorte and C. B. Murray, *J. Am. Chem. Soc.*, 2015, **137**, 6906–6911.
19 D. Li, C. Wang, D. Tripkovic, S. Sun, N. M. Markovic and V. R. Stamenkovic, *ACS Catal.*, 2012, **2**, 1358–1362.
20 P. Mohapatra, S. Shaw, D. Mendivelso-Perez, J. M. Bobbitt, T. F. Silva, F. Naab, B. Yuan, X. Tian, E. A. Smith and L. Cademartiri, *Nature Commun.*, 2017, **8**, 1–7.
21 Y. Altowairqi, A. Alsubaie, K. P. Stroh, I. G. Perez-Marin, L. Bowen, M. Szablewski and D. P. Halliday, *Mater. Today*, 2019, **18**, 473–486.
22 J. F. Chang, W. C. Lin and M. H. Hon, *Appl. Surf. Sci.*, 2001, **183**, 18–25.
23 S. Shaw, J. L. Colaux, J. L. Hay, F. C. Peiris and L. Cademartiri, *Adv. Mater.*, 2016, **28**, 8900–8905.
24 S. Shaw, X. Tian, T. F. Silva, J. M. Bobbitt, F. Naab, C. L. Rodrigues, E. A. Smith and L. Cademartiri, *Chem. Mater.*, 2018, **30**, 5961–5967.
25 L. Wang, B. Zhang and Q. Rui, *ACS Catal.*, 2018, **8**, 10564–10572.
26 A. Hassinen, I. Moreels, K. De Nolf, P. F. Smet, J. C. Martins and Z. Hens, *J. Am. Chem. Soc.*, 2012, **134**, 20705–20712.
27 R. R. Knauf, J. C. Lennox and J. L. Dempsey, *Chem. Mater.*, 2016, **28**, 4762–4770.
28 M. L. Kessler, H. E. Starr, R. R. Knauf, K. J. Rountree and J. L. Dempsey, *Phys. Chem. Chem. Phys.*, 2018, **20**, 23649–23655.
29 A. Ritchhart and B. M. Cossairt, *Inorg. Chem.*, 2019, **58**, 2840–2847.
30 M. Sluydts, K. De Nolf, V. Van Speybroeck, S. Cottenier and Z. Hens, *ACS Nano*, 2016, **10**, 1462–1474.
31 A. Nag, M. V. Kovalenko, J. S. Lee, W. Y. Liu, B. Spokoyny and D. V. Talapin, *J. Am. Chem. Soc.*, 2011, **133**, 10612–10620.
32 M. Kovalenko, M. Scheele and D. Talapin, *Science*, 2009, **324**, 1417–1420.
33 A. Fafarman, W. Koh, B. Diroll, D. Kim, D.-K. Ko, S. Oh, X. Ye, V. Doan-Nguyen, M. Crump, D. Reifsnyder, C. Murray and C. Kagan, *J. Am. Chem. Soc.*, 2011, **133**, 15753–15761.
34 J. Z. Fan, N. T. Andersen, M. Biondi, P. Todorović, B. Sun, O. Ouellette, J. Abed, L. K. Sagar, M.-J. Choi, S. Hoogland, F. P. G. de Arquer and E. H. Sargent, *Adv. Mater.*, 2019, **31**, 1904304.
35 B. Hughes, D. Ruddy, J. Blackburn, D. Smith, M. Bergren, A. Nozik, J. Johnson and M. Beard, *ACS Nano*, 2012, 120509235448008.
36 N. C. Anderson, M. P. Hendricks, J. J. Choi and J. S. Owen, *J. Am. Chem. Soc.*, 2013, **135**, 18536–18548.
37 D. C. Gary, A. Petrone, X. Li and B. M. Cossairt, *Chem. Commun.*, 2016, **53**, 161–164.
38 D. A. Henckel, O. Lenz and B. M. Cossairt, *ACS Catal.*, 2017, **7**, 2815–2820.
39 A. Nelson, Y. Zong, K. E. Fritz, J. Suntivich and R. D. Robinson, *ACS Materials Lett.*, 2019, **1**, 177–184.
40 D. Ung and B. M. Cossairt, *ACS Appl. Energy Mater.*, 2019, **2**, 1642–1645.
41 N. C. Anderson and J. S. Owen, *Chem. Mater.*, 2013, **25**, 69–76.
42 A. Dong, X. Ye, J. Chen, Y. Kang, T. Gordon, J. M. Kikkawa and C. B. Murray, *J. Am. Chem. Soc.*, 2011, **133**, 998–1006.
43 S. E. Doris, J. J. Lynch, C. Li, A. W. Wills, J. J. Urban and B. A. Helms, *J. Am. Chem. Soc.*, 2014, **136**, 15702–15710.
44 J. S. Owen, J. Park, P. Trudeau and A. P. Alivisatos, *J. Am. Chem. Soc.*, 2008, **130**, 12279–12281.
45 Z. Ning, Y. Ren, S. Hoogland, O. Voznyy, L. Levina, P. Stadler, X. Lan, D. Zhitomirsky and E. H. Sargent, *Adv. Mater.*, 2012, **24**, 6295–6299.
46 H. Zhang, J. Jang, W. Liu and D. V. Talapin, *ACS Nano*, 2014, **8**, 7359–7369.
47 M. V. Kovalenko, M. I. Bodnarchuk, J. Zaumseil, J.-S. Lee and D. V. Talapin, *J. Am. Chem. Soc.*, 2010, **132**, 10085–10092.
48 X. Chen and A. R. McDonald, *Adv. Mater.*, 2016, **28**, 5738–5746.
49 S. S. Chou, M. De, J. Kim, S. Byun, C. Dykstra, J. Yu, J. Huang and V. P. Dravid, *J. Am. Chem. Soc.*, 2013, **135**, 4584–4587.
50 L. Zhou, B. He, Y. Yang and Y. He, *RSC Adv.*, 2014, **4**, 32570–32578.
51 K. C. Knirsch, N. C. Berner, H. C. Nerl, C. S. Cucinotta, Z. Gholamvand, N. McEvoy, Z. Wang, I. Abramovic, P. Vecera, M. Halik, S. Sanvito, G. S. Duesberg, V. Nicolosi, F. Hauke, A. Hirsch, J. N. Coleman and C. Backes, *ACS Nano*, 2015, **9**, 6018–6030.
52 E. E. Benson, H. Zhang, S. A. Schuman, S. U. Nanayakkara, N. D. Bronstein, S. Ferrere, J. L. Blackburn and E. M. Miller, *J. Am. Chem. Soc.*, 2018, **140**, 441–450.
53 D. Voiry, A. Goswami, R. Kappera, C. de C. C. e Silva, D. Kaplan, T. Fujita, M. Chen, T. Asefa and M. Chhowalla, *Nature Chem.*, 2015, **7**, 45–49.
54 J. I. Paredes, J. M. Munuera, S. Villar-Rodil, L. Guardia, M. Ayán-Varela, A. Pagán, S. D. Aznar-Cervantes, J. L. Cenis, A. Martínez-Alonso and J. M. D. Tascón, *ACS Appl. Mater. Interfaces*, 2016, **8**, 27974–27986.
55 E. X. Yan, M. Cabán-Acevedo, K. M. Papadantonakis, B. S. Brunschwig and N. S. Lewis, *ACS Materials Lett.*, 2020, **2**, 133–139.
56 A. Hirsch and F. Hauke, *Angew. Chem. Int. Ed.*, 2018, **57**, 4338–4354.
57 M. S. Strano, C. A. Dyke, M. L. Usrey, P. W. Barone, M. J. Allen, H. Shan, C. Kittrell, R. H. Hauge, J. M. Tour and R. E. Smalley, *Science*, 2003, **301**, 1519–1522.
58 Z. Sofer, J. Luxa, D. Bouša, D. Sedmidubský, P. Lazar, T. Hartman, H. Hardtdegen and M. Pumera, *Angew. Chem. Int. Ed.*, 2017, **56**, 9891–9896.
59 J. Greeley, T. F. Jaramillo, J. Bonde, I. Chorkendorff and J. K. Nørskov, *Nature Mater.*, 2006, **5**, 909–913.
60 Z. W. Seh, J. Kibsgaard, C. F. Dickens, I. Chorkendorff, J. K. Nørskov and T. F. Jaramillo, *Science*, 2017, **355**, eaad4998.
61 A. Cirri, A. Silakov, L. Jensen and B. J. Lear, *J. Am. Chem. Soc.*, 2016, **138**, 15987–15993.
62 D. Eguchi, M. Sakamoto and T. Teranishi, *Chem. Sci.*, 2017, **9**, 261–265.
63 C. Chu, D. Huang, Q. Zhu, E. Stavitski, J. A. Spies, Z. Pan, J. Mao, H. L. Xin, C. A. Schmuttenmaer, S. Hu and J.-H. Kim, *ACS Catal.*, 2019, **9**, 626–631.
64 Y.-H. Chung, D. Y. Chung, N. Jung and Y.-E. Sung, *J. Phys. Chem. Lett.*, 2013, **4**, 1304–1309.
65 Y.-H. Chung, S. J. Kim, D. Y. Chung, H. Y. Park, Y.-E. Sung, S. J. Yoo and J. H. Jang, *Chem. Commun.*, 2015, **51**, 2968–2971.
66 C. Kim, T. Eom, M. S. Jee, H. Jung, H. Kim, B. K. Min and Y. J. Hwang, *ACS Catal.*, 2017, **7**, 779–785.
67 Z. Wang, K. Sun, C. Liang, L. Wu, Z. Niu and J. Gao, *ACS Appl. Energy Mater.*, 2019, **2**, 192–195.

68 Z. Cao, D. Kim, D. Hong, Y. Yu, J. Xu, S. Lin, X. Wen, E. M. Nichols, K. Jeong, J. A. Reimer, P. Yang and C. J. Chang, *J. Am. Chem. Soc.*, 2016, **138**, 8120–8125.
69 S. G. Kwon, G. Krylova, A. Sumer, M. M. Schwartz, E. E. Bunel, C. L. Marshall, S. Chattopadhyay, B. Lee, J. Jellinek and E. V. Shevchenko, *Nano Lett.*, 2012, **12**, 5382–5388.
70 J. R. Pankhurst, Y. T. Guntern, M. Mensi and R. Buonsanti, *Chem. Sci.*, 2019, **10**, 10356–10365.
71 M. Zobel, R. B. Neder and S. A. J. Kimber, *Science*, 2015, **347**, 292–294.
72 Y. Li and C. Zhao, *ACS Catal.*, 2017, **7**, 2535–2541.
73 W. Gao, W. Gou, X. Zhou, J. C. Ho, Y. Ma and Y. Qu, *ACS Appl. Mater. Interfaces*, 2018, **10**, 1728–1733.
74 G.-R. Xu, J. Bai, L. Yao, Q. Xue, J.-X. Jiang, J.-H. Zeng, Y. Chen and J.-M. Lee, *ACS Catal.*, 2017, **7**, 452–458.
75 Y. Ding, B.-Q. Miao, Y.-C. Jiang, H.-C. Yao, X.-F. Li and Y. Chen, *J. Mater. Chem. A*, 2019, **7**, 13770–13776.
76 P. Liu and J. A. Rodriguez, *J. Am. Chem. Soc.*, 2005, **127**, 14871–14878.
77 L. S. Byskov, M. Bollinger, J. K. Nørskov, B. S. Clausen and H. Topsøe, *J. Molec. Catal. A*, 2000, **163**, 117–122.
78 J. V. Lauritsen, M. V. Bollinger, E. Lægsgaard, K. W. Jacobsen, J. K. Nørskov, B. S. Clausen, H. Topsøe and F. Besenbacher, *J. Catal.*, 2004, **221**, 510–522.
79 M. F. Delley, Z. Wu, M. E. Mundy, D. Ung, B. M. Cossairt, H. Wang and J. M. Mayer, *J. Am. Chem. Soc.*, 2019, **141**, 15390–15402.
80 M. N. Jackson, C. J. Kaminsky, S. Oh, J. F. Melville and Y. Surendranath, *J. Am. Chem. Soc.*, 2019, **141**, 14160–14167.
81 M. N. Jackson, M. L. Pegis and Y. Surendranath, *ACS Cent. Sci.*, 2019, **5**, 831–841.
82 M. N. Jackson and Y. Surendranath, *Acc. Chem. Res.*, 2019, **52**, 3432–3441.

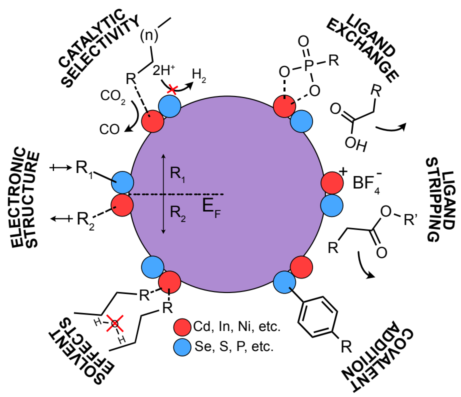

Interfacial chemistry dramatically impacts the activity (performance) and reactivity (mechanism) of nanoparticle catalysts.